THE JOURNAL OF PHYSICAL CHEMISTRY B

Article

pubs.acs.org/JPCB

A T-Shaped Amphiphilic Molecule Forms Closed Vesicles in Water and Bicelles in Mixtures with a Membrane Lipid

Peggy Scholtysek,[†] Anja Achilles,[‡] Claudia-Viktoria Hoffmann,[†] Bob-Dan Lechner,[†] Annette Meister,[§] Carsten Tschierske,[⊥] Kay Saalwächter,[‡] Katarina Edwards,[¶] and Alfred Blume*[,†]

[†]Institute of Chemistry - Physical Chemistry, Martin-Luther-University Halle-Wittenberg, D-06120, Halle/Saale, Germany

[‡]Institute of Physics - NMR, Martin-Luther-University Halle-Wittenberg, D-06120, Halle/Saale, Germany

[§]ZIK HALOmem, Martin-Luther-University Halle-Wittenberg, D-06120, Halle/Saale, Germany

[⊥]Institute of Chemistry - Organic Chemistry, Martin-Luther-University Halle-Wittenberg, D-06120, Halle/Saale, Germany

[¶]Institute for Physical and Analytical Chemistry, Uppsala University, 75123 Uppsala, Sweden

Supporting Information

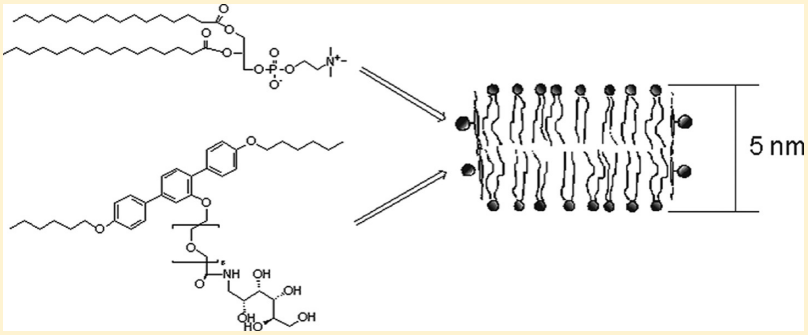

ABSTRACT: The T-shaped amphiphilic molecule A6/6 forms a columnar hexagonal liquid-crystalline phase between the crystalline and the isotropic liquid when studied in bulk (Chen et al., 2005). Because of the hydrophilic and flexible oligo(oxyethylene) side chain terminated by a 1-acylamino-1-deoxy-D-sorbitol moiety attached to a rigid terphenyl core with terminal hexyloxy alkyl chains, it was expected that also formation of lyotropic phases could be possible. We therefore studied the behavior of A6/6 in water and also in mixtures with bilayer-forming phospholipids, such as dipalmitoyl-phosphatidylcholine (DPPC), using differential scanning calorimetry (DSC), transmission electron microscopy (TEM), cryo-transmission electron microscopy (cryo-TEM), dynamic light scattering (DLS), and solid-state nuclear magnetic resonance (ssNMR). DSC showed for the pure A6/6 suspended in water a phase transition at ca. 23 °C. TEM and cryo-TEM showed vesicular as well as layered structures for pure A6/6 in water below and above this phase transition. By atomic force microscopy (AFM), the thickness of the layer was found to be 5−6 nm. This leads to a model for a bilayer formed by A6/6 with the laterally attached polar side chains shielding the hydrophobic layer built up by the terphenyl core with the terminal alkyl chains of the molecules. For DPPC:A6/6 mixtures (10:1), the DSC curves indicated a stabilization of the lamellar gel phase of DPPC. Negative staining TEM and cryo-TEM images showed planar bilayers with hexagonal morphology and diameters between 50 and 200 nm. The hydrodynamic radius of these aggregates in water, investigated by dynamic light scattering (DLS) as a function of time and temperature, did not change indicating a very stable aggregate structure. The findings lead to the proposition of a new bicellar structure formed by A6/6 with DPPC. In this model, the bilayer edges are covered by the T-shaped amphiphilic molecules preventing very effectively the aggregation to larger structures.

INTRODUCTION

The complex composition of biological membranes necessitates the use of model membrane systems to investigate bilayer properties.[2−4] Liposomes or lipid vesicles are usually used as model systems because they can be easily prepared. However, bicelles are also a promising model system particularly in the field of NMR on lipid−protein interactions. Bicelles typically consist of a phospholipid with long fatty acid chains like 1,2-dimyristoyl-*sn*-glycero-3-phosphatidylcholine (DMPC) forming the plane bilayer fragment and a shorter lipid like 1,2-dihexanoyl-*sn*-glycero-3-phosphatidylcholine (DHPC) aligning at the edges and stabilizing these disk-shaped aggregates. The shorter lipid can also be replaced by bile salts or peptides as reported previously.[5,6] Bicelles combine properties of lipid bilayers and micelles and offer a possibility to investigate membrane-binding molecules like, for example, integral

Received: August 19, 2011
Revised: March 2, 2012
Published: April 6, 2012

Scheme 1. (a) T-Shaped Amphiphile A6/6 and (b) 1,2-Dipalmitoyl-*sn*-glycero-3-phosphocholine (DPPC)

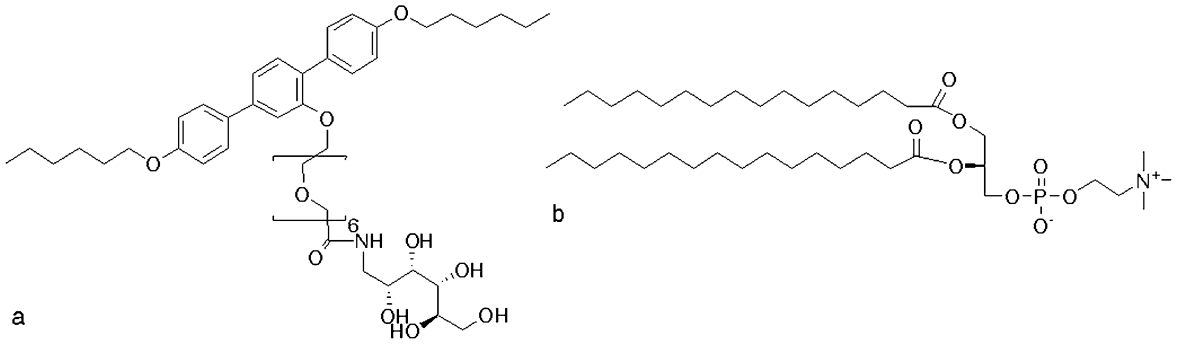

membrane proteins in contact with planar lipid bilayers.[5−10] Furthermore, the penetration of bicelles into skin has been studied, and it was shown that the fusion of bicelles with skin lipids can change their lamellar order depending on the chain length of the phospholipid.[11] Bicelles are also easily alignable in a magnetic field and can be analyzed using solid-state and solution nuclear magnetic resonance (NMR).[5] Despite the fact that well-established bicellar systems exist, it is important to find other bicelle-forming systems containing compounds having no detergent-like action because the presence of detergents at the rim of the bicelles might influence the behavior of peptides or proteins incorporated or bound to the bicelles.[12,13]

The compound A6/6 (see Scheme 1 a) is a polyhydroxy alkyl amide which is built up of a rodlike hydrophobic terphenyl core with two predominantly hydrophobic and flexible terminal hexyloxy alkyl chains.[1] The notation A*m*/*n* describes the general design of this kind of facial amphiphilic molecule where the lateral side chain is connected to the central phenyl ring of the core. m = 6 is the number of hydrocarbon units of the flexible terminal side chains and n = 6 is the number of oxyethylene units within the lateral side chain. The bulky hydrophilic lateral oligo(oxyethylene) chain is terminated by a carbohydrate derivative (see Scheme 1 a). A6/6 exhibits amphotropic behavior. With changing temperature, the formation of a thermotropic mesophase can be detected for the bulk sample. Below −6 °C, A6/6 exists in a glassy state. Above this temperature, a liquid crystalline columnar hexagonal Col_h (*p6mm*) phase appears and is stable up to a temperature of 102 °C, where an isotropic melt is formed.[1] These facial amphiphiles were studied in recent years in detail for their mesophase behavior,[1,14−16] and also the behavior of monomolecular films at the air/water interface was extensively investigated.[17−19] We selected A6/6 as a compound to study its interaction with phospholipid bilayers made from 1,2-dipalmitoyl-*sn*-glycero-3-phosphocholine (DPPC) to elucidate the possibility that in mixtures of A6/6 with DPPC bicelles are formed.

DPPC is a well-studied phospholipid because of its importance and frequency of occurrence in biological membranes.[20] It is also one of the constituents of the monolayer covering and protecting pulmonary alveoli from collapse during respiration.[21−23] The lipid is built up by a glycerol backbone structure to which saturated fatty acids are connected at the *sn*-1 and *sn*-2 positions. The hydrophilic part of the molecule is a phosphocholine group connected to the *sn*-3 position of the glycerol (see Scheme 1 b). The lyotropic and thermotropic behavior of DPPC is well characterized as it serves as a model system for biological membranes. Summarizing briefly its lyotropic behavior, DPPC in excess water forms several different lamellar phases. At temperatures below 41 °C, it forms the so-called gel phases with ordered lipid chains with the phase sequence L_c => $L_{\beta'}$ => $P_{\beta'}$, and above this main transition temperature, the molecules have disordered chains when they are in the liquid-crystalline L_α-phase.

In this work, we describe the results of studies of the lyotropic behavior of A6/6 and its interaction with the bilayer-forming phospholipid DPPC. The first aim of our study was to investigate how A6/6 self-assembles by itself when suspended in water. Because of the large hydrophilic lateral side chain of A6/6, we expected to find also lyotropic phase behavior for this amphiphile. The second question was how it changes the lipid aggregate structure when mixed with a phospholipid. Because of the completely different shape of A6/6 compared to the bilayer-forming DPPC, it was unclear whether A6/6 would be incorporated into the bilayer or not. We therefore wanted to test whether these amphiphiles with lateral side chains would perforate the lipid bilayer by aggregating inside the bilayer to form holes or whether they would change the aggregation behavior in a completely different way, namely, in the form of bicelles or other possible structures.

We will show here that A6/6 by itself forms unexpected lyotropic aggregate structures. When mixed with DPPC, we could show that vesicular structures are not stable but that planar aggregates are formed instead, which adopt the form of bicellar-like structures being very stable as a function of time and temperature. This new bicellar system might offer new possibilities for studying interactions of molecules with membranes using, for instance, NMR techniques.

EXPERIMENTAL SECTION

Materials. 1,2-Dipalmitoyl-*sn*-glycero-3-phosphocholine (DPPC) was purchased from Genzyme Pharmaceuticals (Liestal, Switzerland) with purity >99% and was used without further purification. A6/6 (*N*-[(2S,3R,4R,5R)-2,3,4,5,6-pentahydroxyhexyl]-20-(4,4″-dihexyloxy-p-terphenyl-2′-yl-oxy)-3,6,9,12,15,18-hexaoxaeicosanoylamide) was synthesized as described previously.[1] A6/6 was dried in a vacuum-drying cabinet at about 60 °C for at least 3 h before use.

Experiments were performed with ultrapure water of Millipore quality (conductivity < 0.055 μS/cm; total organic carbon (TOC) < 5 ppm).

Differential Scanning Calorimetry (DSC). The temperature-dependent behavior of pure A6/6 and DPPC:A6/6 mixtures was investigated using a VP-DSC microcalorimeter (MicroCal, Inc. Northhampton, United States). Aliquots from stock solutions of A6/6 and DPPC in chloroform were mixed

dx.doi.org/10.1021/jp207996r | J. Phys. Chem. B 2012, 116, 4871−4878

in the appropriate amounts in a vial. The organic solvent was evaporated at higher temperature, and the lipid film was dried under vacuum. The aqueous suspensions with a concentration of 2 mM were prepared by adding the desired amount of ultrapure water, by vortexing at high temperature, and then by sonicating the sample in a bath type sonicator for 1 h at 60−70 °C. The degassed suspension was filled into the sample cell of the calorimeter, and the reference cell was filled with pure water. The experiments were performed with a heating and cooling rate of 60 K/h in a temperature interval between 5 and 60 °C because no transitions could be detected above this temperature. Several scans were performed to test for reproducibility. The water baseline was subtracted from the sample thermogram, and the resulting difference curve was analyzed using the ORIGIN software supplied by MicroCal. The scans shown in the figures represent the fourth heating curve of each sample.

Transmission Electron Microscopy (TEM) and Cryo-Transmission Electron Microscopy (cryo-TEM). For TEM using negative staining, 5 μL of the aqueous suspensions (0.05 mg/mL or 0.1 mg/mL) of A6/6 and the DPPC:A6/6 = 10:1 mixture, respectively, were spread onto Cu grids with a diameter of 3 mm coated with a Formvar film, were blotted, were stained with 5 μL of 1% uranyl acetate solution, and subsequently blotted and dried. The grids were prepared and dried at a temperature 3−5 °C in a cold room or at room temperature, respectively, and then were viewed using a Zeiss EM 900 transmission electron microscope.

Cryo-TEM grids were prepared similarly as for TEM. Specimens were prepared by a blotting procedure performed in a chamber with controlled temperature and humidity. A drop of the sample solution (0.1 mg/mL) was placed onto an EM grid coated with a perforated polymer film. Excess solution was then removed with a filter paper leaving a thin film of the solution spanning the holes of the polymer film on the EM grid. Vitrification of the thin film was achieved by rapid plunging of the grid into liquid ethane held just above its freezing point. The vitrified specimen was kept below 108 K during both transfers to the microscope and the investigation. Measurements were performed immediately after preparation of the grids with a Zeiss 902 A microscope operating at 80 kV.

Dynamic Light Scattering (DLS). Dynamic light scattering measurements were performed with an ALV-NIBBS/HPPS High Performance Particle Sizer (ALV Laser Vertriebsgesellschaft mbH, Langen, Germany). The aqueous suspensions of A6/6 and mixtures of lipid and A6/6 were poured into 1 mL Plexiglas cells and were heated to 50 °C. The hydrodynamic radii were calculated using the CONTIN software provided by ALV.

Solid-State Nuclear Magnetic Resonance (ssNMR). ^{13}C detected solid-state NMR was used to examine the dynamics of the lipid molecules in the presence of A6/6. To investigate these dynamics, we used a two-dimensional DIPSHIFT-like experiment, which is described elsewhere.[24] Because of the fast molecular motion of the lipid molecules,[25] the $^{13}C-^{1}H$ heteronuclear dipolar coupling, which is the crucial parameter for this experiment, is either averaged out completely (isotropic mobility) or averaged to a rather large extent (anisotropic mobility). Therefore, it is complicated to estimate this weak residual coupling by the frequently employed DIPSHIFT sequence.[26]

The sequence applied here is a further development of the original DIPSHIFT experiment. The idea is to recouple the heteronuclear dipolar interaction by means of additional pi-pulses as known from the REDOR sequence.[27] The recoupling yields an amplification of the dipolar interaction, which leads to a stronger apparent residual dipolar coupling as described in Hong et al.[28] Thus, by measuring this residual dipolar coupling (D_{res}) and by comparing it to the static-limit value (D_{stat}), a dynamic order parameter can be obtained as described by

$$S = \langle D_{res} \rangle / D_{stat}$$

Hence, this dynamic order parameter characterizes the local degree of anisotropy of the molecular motion, where $S = 0$ means the motion is completely isotropic and $S = 1$ results from a rigid sample.

The NMR experiments were performed on a Bruker Avance III 400 spectrometer with resonance frequencies of 400 and 100.5 MHz for ^{1}H and ^{13}C, respectively. All experiments were carried out on a 4 mm double resonance probe at a spinning frequency of 5 kHz. For temperature-dependent measurements, the sample temperature was calibrated[29,30] and is accurate within ±1 K. The used 90° pulse lengths were 3.2 and 3 μs for protons and ^{13}C, respectively. To avoid decoupling-induced sample heating,[31] a recycle delay of 5 s was used. Samples for NMR measurements were prepared by adding 50 wt % of deuterated water to the powder samples in the NMR rotor to retain the phase transitions measured by DSC.

RESULTS AND DISCUSSION

Differential Scanning Calorimetry (DSC). Calorimetric investigations of the pure substances and various DPPC:A6/6 mixtures in aqueous suspensions were performed to test for the lyotropic behavior of pure A6/6 and the mixtures. Pure A6/6 can be suspended in water giving an almost clear solution. When the aqueous suspension is heated during the DSC scan, peaks at 15.3 °C and a higher one at 21.5 °C can be detected indicating transitions between lyotropic phases of different order (see Figure 1). The structure of the lyotropic phases and the nature of the phase transitions of A6/6 in water are not clear at present. For the pure DPPC, the well-known main phase transition from the gel to the liquid-crystalline phase is observed at 41.8 °C (see Figure 1).[2,3,32−34]

The thermograms observed for the mixtures of DPPC:A6/6 with a high lipid ratio (100:1 and 50:1) show that A6/6 can be incorporated into the bilayer and leads to a broadening of the phase transition and to a slight shift to lower temperature. The peaks for mixtures with higher content of A6/6, that is, for the 20:1 and 10:1 ratios, are in contrast shifted to slightly higher temperatures and are separated into two maxima with temperatures at 40.5 and 43.5 °C. This can be interpreted on the one hand as a stabilization of the gel phase. On the other hand, a phase separation of almost pure DPPC seems to occur which can be deduced from the appearance of a transition peak at 41 °C. The high-temperature peak remains in all mixtures at the same position up to a mixing ratio of 1:1. The mixture with mixing ratios 4:1, 2:1, and 1:1 exhibit additionally a small peak at about 20−23 °C, which possibly indicates a phase separation of pure A6/6. Furthermore, an additional small sharp peak is seen at ca. 34 °C. The thermogram thus indicates the presence of various phases of different composition and a complicated thermotropic phase behavior.

Transmission Electron Microscopy (TEM) and Cryo-Transmission Electron Microscopy (cryo-TEM) of A6/6 Aggregates in Water. To elucidate the nature of the lyotropic phases and the morphology of the aggregates formed

dx.doi.org/10.1021/jp207996r | J. Phys. Chem. B 2012, 116, 4871−4878

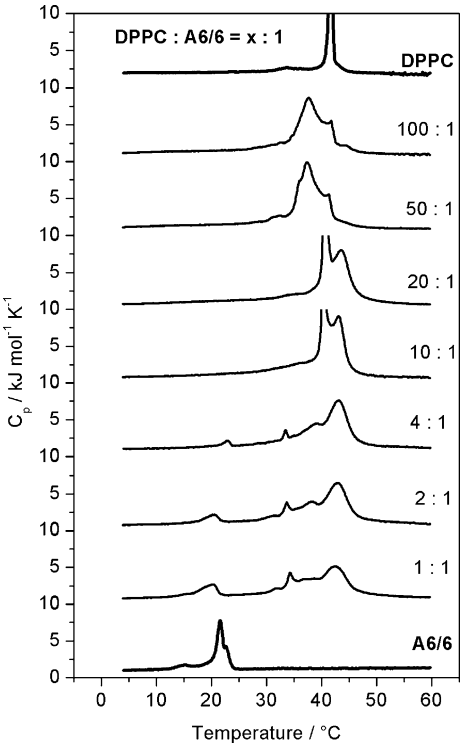

Figure 1. Heating curves of the mixtures DPPC:A6/6 = *x*:1 with different mixing ratios. Total concentration was 2 mM.

when A6/6 is dispersed in water, we took TEM images of pure A6/6 suspensions using negative staining electron microscopy. A6/6 suspended in water without and with previous sonication was imaged after staining and drying. Nonsonicated solutions prepared at 5 °C below the transition as detected by DSC showed lamellar structures of different widths which are several micrometers in length and which look like folded sheets because of the blotting and drying procedure (see Figure 2 a, b). The edges of the sheets are perfectly smooth and straight indicating a well-ordered structure of the molecules in the lamellae. The surface of the lamellae seems to be very smooth as hardly any defects are seen, and the thickness of the sheets seems to be the same for all aggregates. As described above, A6/6 shows a major thermotropic transition in water at ca. 23 °C. We therefore also imaged samples prepared above this transition temperature. In Figure 2 c and d, collapsed vesicular structures can be seen with sizes up to several micrometers in diameter. The crinkling of the structures is a consequence of the drying process during sample preparation but indicates that the lamellar structure becomes more flexible above the transition at 23 °C.

Sonication of the aqueous A6/6 suspension breaks up the larger aggregates and leads to the formation of other types of aggregate structures (see Figure 3). The morphology found for samples prepared at 5 °C is shown in Figure 3 a and b. In Figure 3a, circular structures with diameters somewhat larger than 500 nm can be seen looking like ruptured and flattened vesicles. The smaller structures with dimensions of about 100–300 nm seem to be folded lamellae. Additionally, we found fibers with lengths up to a few micrometers (see Figure 3 b).

When the sample preparation of the sonicated suspension was performed at room temperature above the transition of A6/6 detected by DSC, images as shown in Figure 3 c and d with quite similar structures were seen. Again, we found circular

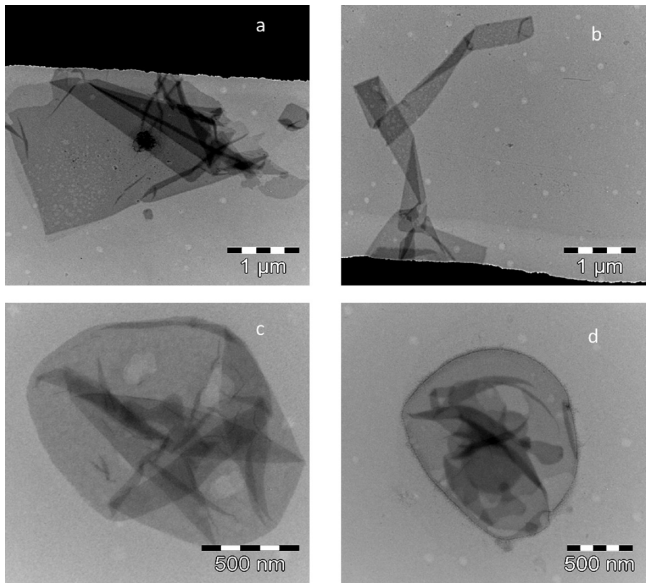

Figure 2. TEM images of A6/6 from aqueous suspension without previous sonication. Grids in a and b were prepared at 5 °C; lamellar structures are seen. Grids in c and d were prepared at room temperature above the transition of A6/6 detected by DSC; collapsed vesicular structures are visible.

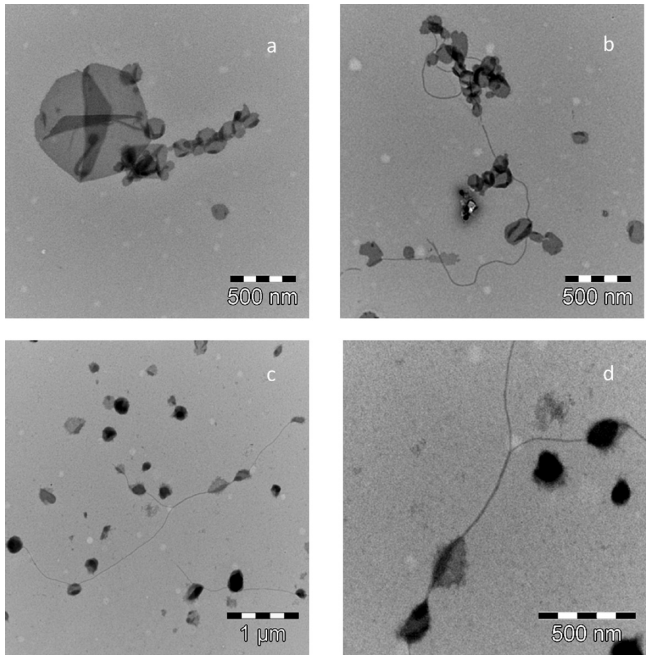

Figure 3. TEM images of A6/6 from aqueous suspension after previous sonication. (a, b) Grids prepared at 5 °C. (c, d) Grids prepared at room temperature above the transition of A6/6 detected by DSC.

structures looking like folded lamellae, and additionally we found long fibers. The lamellar and fiber structures seem to be more flexible than at lower temperature.

Because transmission electron microscopy with negative staining is not free from artifacts and because the drying procedure leads to an orientation of objects parallel to the Formvar surface on the grid preventing the analysis of the 3-D structure, cryo-TEM was used in addition. This is an imaging technique which gives also hints on the three-dimensional

dx.doi.org/10.1021/jp207996r | J. Phys. Chem. B 2012, 116, 4871–4878

morphology of the aqueous sample after vitrification. Figure 4 shows two representative images of the morphology of a

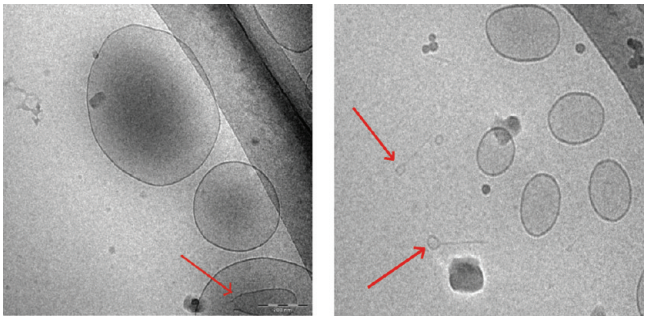

Figure 4. Cryo-TEM images of A6/6 in water; mostly unilamellar vesicles are observed. Left: red arrow points to an open vesicle. Right: red arrows point to small unilamellar vesicles with attached fibers. Grids were quenched from 25 °C. Scale bars: 200 nm.

sonicated A6/6 sample prepared at 25 °C. For pure A6/6 at room temperature, we observe mostly unilamellar vesicles. This structure can be deduced from the higher electron density at the edges of the aggregates. The diameter of the vesicles ranges from 100 to 500 nm. These findings confirm the previous assumption that the crinkled structures found with TEM with negative staining are indeed folded vesicles. Also in Figure 4, small unilamellar vesicles with diameters around 50 nm can be seen with 200 nm long fibers attached to them. The fiber structures here are shorter than those observed in the TEM images with negative staining (see Figure 3). Overall, however, the cryo-TEM images support the previous finding with negative staining TEM that A6/6 forms mainly closed structures with a continuous layer of molecules.

In the unilamellar sheets and vesicles, the hydrophobic parts of the molecules are in the middle of the layer and are shielded from water by the hydrophilic groups on both sides of the hydrophobic inner layer formed by the terphenyl moieties and the hexyl chains. Similarly, the fiber cores are made up from the long hydrophobic backbones of the molecules, and the outside is covered by the hydrated hydrophilic groups shielding the inner core from contact with bulk water. Below the phase transition, when the sheets and fibers become more rigid, the terphenyls should adopt an organization preferably parallel to each other. However, whether the terphenyls really adopt a preferred organization parallel to the layers/fibers (see Scheme 2) as typically observed for T-shaped amphiphiles with large lateral groups (Lam phases[15]/axial bundle phases[35]) or perpendicular to them (as in the channeled layer phases and smectic phases[1,16] observed for T-shaped amphiphiles with relatively short chains) cannot be concluded with certainty. However, because the thickness of the sheets determined by

Scheme 2. Left: Schematic Model of A6/6 Aggregation in Aqueous Suspension. Right: Molecular Model of the Possible Lamellar Arrangement of A6/6 Molecules within the Layers with a Hydrophobic Inner Core[a]

[a]The thickness of the layer is 5 to 6 nm.

atomic force microscopy (AFM) (see Figure S1 in the Supporting Information) is only about 5 to 6 nm, an organization of the long terphenyls on average parallel to the layers, as shown in Scheme 2, appears more likely. This mode of organization also provides a better segregation of lipophilic cores and polar lateral chains and is in line with previous observations that large lateral chains favor this kind of organization in bulk liquid-crystalline (LC) phases.[15] In this structure, the rigid terphenyls contribute to the stabilization of the layers/fibers by their parallel alignment. This seems even to be the case when the orientational order becomes only short-range in the more fluid structures above the phase transition.[36]

Transmission Electron Microscopy (TEM) and Cryo-Transmission Electron Microscopy (cryo-TEM) of DPPC:A6/6 Aggregates. We investigated the aggregation behavior of mixtures of A6/6 with DPPC. The TEM images in Figure 5 were obtained with negative staining and show the

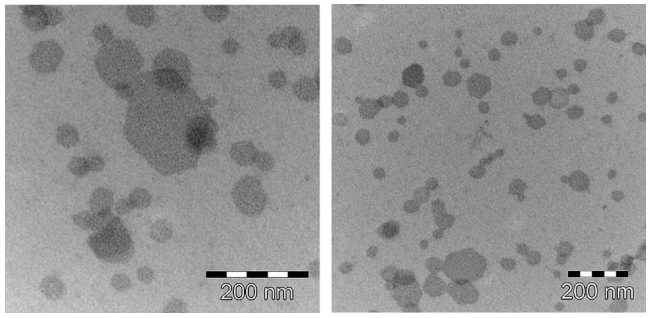

Figure 5. TEM images of the mixture DPPC:A6/6 = 10:1; planar hexagonal discs are visible. Samples were prepared at 5 °C.

aggregates of a mixture of DPPC:A6/6 = 10:1 in water prepared at 5 °C. Planar hexagonal structures with dimensions of 50−200 nm are seen. All aggregates have a similar shape and show similar contrast. We can conclude again that the molecules are arranged in a sheetlike structure. The hexagonal shape of the sheetlike aggregates is probably because DPPC at low temperature is in the lamellar gel phase with tilted acyl chains packed in a hexagonal lattice. The aggregates are therefore most probably rigid bicellar-like structures with the A6/6 molecules located at the edges shielding the hydrophobic surfaces.

To preclude that the images obtained from TEM using negative staining were due to artifacts from the preparation procedure of the samples, the mixture DPPC:A6/6 = 10:1 was also investigated using cryo-TEM. Here, the samples are rapidly quenched to very low temperature and are viewed in transmission without additional contrast agent. The cryo-TEM images shown in Figure 6 support the assumption that indeed bicellar-like structures are formed. The images show planar aggregates either from a top or from a side view. In the side view, the planar aggregates appear as rodlike structures with a higher electron density as compared to the case when viewed from the top. The structures seen in the top view agree with those found with negative staining TEM (see Figure 5). The aggregates have again a diameter of 50−200 nm. For a few of them, even the hexagonal shape due to the hexagonal packing of the fatty acid chains of the phospholipids can be seen.[3,11,37,38] The electron microscopic images therefore clearly show that the mixture of DPPC:A6/6 = 10:1 suspended in water leads to the formation of ordered bicellar-like structures with hexagonal shape.

dx.doi.org/10.1021/jp207996r | J. Phys. Chem. B 2012, 116, 4871−4878

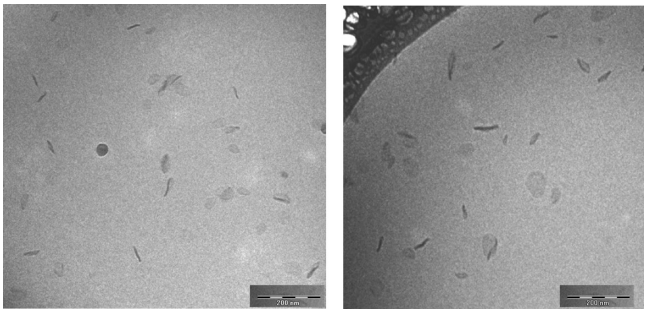

Figure 6. Cryo-TEM images of the mixture DPPC:A6/6 = 10:1 in water; mostly unilamellar bicellelike structures in different orientations are visible. Grids were quenched from 25 °C. Scale bars: 200 nm.

A sketch of the possible molecular arrangement of the molecules in these bicellar-like aggregates is shown in Scheme 3. The nearly T-shaped molecules cover the edges of bilayer

Scheme 3. Proposed Model for the Aggregate of the Mixture DPPC:A6/6 = 10:1 Deduced from the Results of TEM and Cryo-TEM Assuming an Organization of the T-Shaped Facial Amphiphile with Preferred Orientation Parallel to the Lipid Chains in a Staggered Configuration

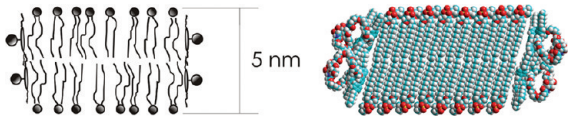

hexagons formed by the phospholipid and, in this way, shield the hydrophobic alkyl chains of the lipids from water. Whether the long axes of the A6/6 molecules are lying parallel or perpendicular to the bilayer normal is not yet certain, but it is more likely that the A6/6 molecules adopt an orientation on average parallel to the main direction of the alkyl chains, that is, perpendicular to the bicellar surface. This would allow the coupling of the main directors of the chains and the rodlike cores as well as a parallel alignment between the rodlike cores allowing the formation of an uninterrupted rim embedding the edges of the bicelles. The maximum length of the hydrophobic unit of A6/6 between the ends of the alkyl chains is 3.1 nm. In the proposed orientation, this would span the major part of the hydrophobic region of the DPPC membrane between the two hydrophilic bicelle surfaces. Staggering of the T-shaped molecules along their long axes as well as in the perpendicular direction (the surface layer becomes slightly thicker than exactly one molecule) provides a complete coverage of the lipophilic bicelle edges by the (hydrated) hydrophilic lateral chains of the densely packed T-shaped amphiphiles.

The size of the bicellar aggregates seen in the TEM images ranges from 50 to 200 nm. We also performed DLS measurements to obtain a better impression of the size distribution. From DLS, we know that the hydrodynamic radii of the mixed systems in water are quite small compared to the aggregates found for the pure substances. For the investigated mixing ratios, the hydrodynamic radii scatter between 18 and 34 nm with an average of ca. 30 nm. Additionally, the aggregates were fairly monodisperse with an average width of the distribution of only 6%. Also, the hydrodynamic radius was more or less the same at a temperature of 50 °C, that is, above the temperature of the highest transition seen by DSC.

The hydrodynamic radius calculated from DLS is based on the assumption of a spherical particle. As we have bicellar-like aggregates, the friction coefficient changes. For an oblate ellipsoid with an axial ratio of 20 (bicelle with r = 50 nm and thickness of 5 nm), the hydrodynamic radius can be calculated from the Perrin equation to ca. 38 nm. For an average apparent hydrodynamic radius of 30 nm observed in our DLS measurements, we can estimate an approximate radius of the bicelle of 40 nm, that is, an average diameter of 80 nm. This is in quite good agreement with the observations by electron microscopy.

The available molecular area per A6/6 molecule surrounding a disk with a radius of r = 50 nm can be easily calculated. A disk of this size would contain ca. 2.6×10^4 molecules of DPPC assuming an area of 0.6 nm^2 per DPPC molecule. For a ratio DPPC:A6/6 = 10:1 (as in our samples), the number of A6/6 molecules at the rim would be 2.6×10^3. The available area at the rim calculated from the circumference and the thickness of the bilayer (5 nm) would amount to $\sim 1.6 \times 10^3$ nm^2. This would lead to an available molecular area of ~0.6 nm^2 for an A6/6 molecule. In monolayer experiments (unpublished results), where A6/6 was spread at the air/water surface and was compressed, we determined an area of ~0.8 nm^2 per A6/6 before film collapse. The calculation for the bicellar system thus shows that enough molecules of A6/6 are available to cover the edges of the bicellar aggregate with a complete monolayer.

The size deviations between electron microscopy images and DLS are normal because of the different observation techniques. DLS measures the ensemble average over a large number of aggregates, whereas only few aggregates are always visible in the EM images making it difficult to obtain a reliable size distribution. A further interesting finding is that the aggregates are stable over time and after many heating and cooling cycles. We compared freshly measured DSC samples with DSC suspensions stored after the calorimetric measurements at 4 °C for a few months. The particle size had stayed almost the same. Additionally, their size did not change considerably by exposing the samples to several temperature cycles from room temperature to 90 °C within the DSC instrument. The hydrodynamic radii from freshly prepared suspensions and from samples after the DSC runs were essentially the same with differences of about 2 to 3 nm.

ssNMR. Solid-state NMR is the method of choice to study the behavior of bicellar-like aggregates concerning their dynamic and structural behavior. This has been recently shown for DMPC/DHPC bicelles.[39,40] To qualitatively probe the influence of A6/6 on the lipid molecules in DPPC, both the pure substances and a 15:1 mixture of DPPC:A6/6 were examined by means of $^{13}C\{^1H\}$ solid-state NMR using a DIPSHIFT experiment under magic angle spinning (MAS) conditions. For this purpose, different experiments were performed for pure DPPC, pure A6/6, and a mixture of both samples with a molar ratio of 15:1 in D_2O at a concentration of 50 wt %. The samples consisted of multilamellar aggregates with random orientation.

In Figure 7, the ^{13}C spectra for the three samples at a temperature of T = 47 °C are shown. We chose this temperature to make sure that the lipid was already in the L_α phase, which is indicated by the narrow peaks in the ^{13}C spectra of the samples. By comparing the spectra of the pure substances and of the mixture, we found an additional peak appearing in the spectrum of the mixture, which we assigned to the oxyethylene chain in the A6/6 molecule (10 CH_2 groups in

dx.doi.org/10.1021/jp207996r | J. Phys. Chem. B 2012, 116, 4871–4878

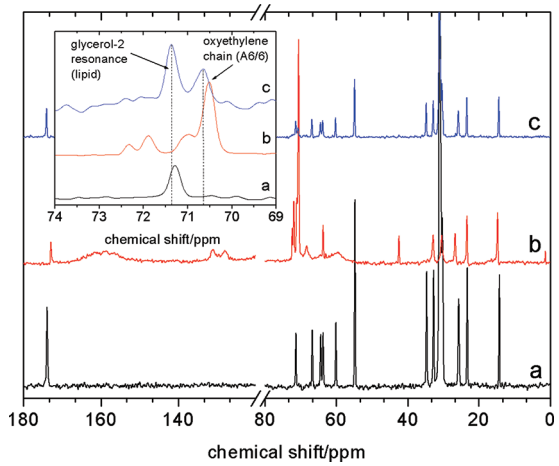

Figure 7. ^{13}C spectra for (a) pure DPPC, (b) pure A6/6, and (c) 15:1 mixture of DPPC:A6/6 for T = 47 °C. In the inset, arrows indicate the selected resonances (glycerol-2 carbon of the lipid and oxyethylene chain of A6/6) for the dynamic measurements.

total). The rest of the resonances from the A6/6 molecule is not observed in the spectrum of the mixture as it contains only a small amount of A6/6 (~3.5 mg). Thus, the resonances are covered by large peaks of the lipid molecule. From the comparison of the spectra, we can say that there are no significant conformational changes in the lipid molecules because such rearrangements would result in a considerable change of the chemical shift.[41] The small change in the chemical shift of the oxyethylene chain of A6/6 is probably due to a slightly different conformation adopted in the pure substance (vesicles) and the mixture (bicelles).

A subset from the dynamics measurements is shown in Figure 8. Here, the DIPSHIFT modulation curves for the glycerol-2 carbon in DPPC and for the oxyethylene carbons in A6/6 (cf. inset in Figure 7, arrows indicate the selected resonances) are shown for both in the pure substances and in the mixture. These experiments also were done at a temperature of 47 °C, that is, in the L_α phase. As the depth of the curve is a measure for the residual dipolar coupling and

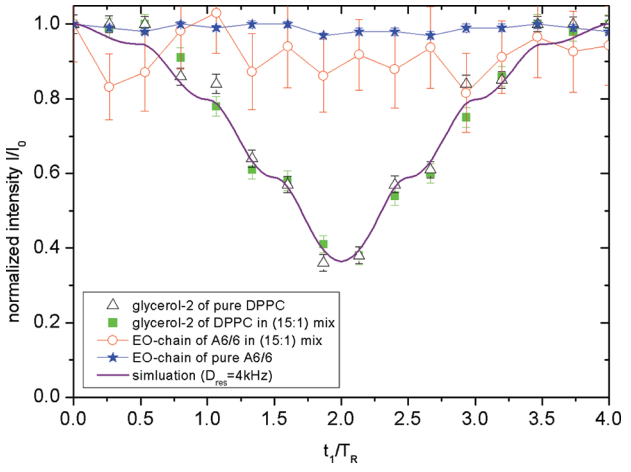

Figure 8. Recoupled DIPSHIFT curves for the glycerol-2 carbon in pure DPPC (open triangles), the 15:1 mixture (squares), and the oxyethylene chain in pure A6/6 (stars) in comparison to the oxyethylene chain in the 15:1 mixture (open circles) at a temperature of T = 47 °C.

therefore a measure for the mobility, we found that the glycerol-2 carbon exhibits the same dynamics in both the pure lipid and the lipid mixed with the A6/6 because they show the same behavior and the same residual dipolar coupling. This can be seen from the simulation of the measured data from which a residual dipolar coupling of $D_{res}/2\pi$ = 4 kHz was obtained. Hence, we estimate the local order parameter to S = 0.18 in the pure lipid and the mixture on the basis of the static limit coupling of a CH group of 22 kHz.

We found these results for all carbons in the DPPC molecule, that is, the curves for the carbons in the mixture show the same trend as the respective carbons in the pure lipid. From this finding, we conclude that the dynamics of the lipid molecules is not influenced by the presence of the A6/6 molecules. Therefore, we deduce that A6/6 is not inserted and distributed homogeneously in the lipid membrane. The same results were obtained in a 75:1 mixture of DPPC:A6/6.

Because the carbons from the oxyethylene chain of the A6/6 molecule constitute a measurable signal in the spectrum of the mixture, their dynamic behavior could also be studied. These measurements are also presented in Figure 8. The curves of this chain in A6/6 are rather flat and thus indicate a nearly isotropic motion as the heteronuclear dipolar coupling is averaged to a near-zero value. For the mixture, we found a similar behavior. The heteronuclear dipolar coupling is also averaged out, but the points are more scattered as compared to the points measured in the pure substance. The reason is the low signal-to-noise ratio as compared to the signal-to-noise ratio in the pure A6/6 sample. Hence, we conclude that the nearly isotropic motion of the oxyethylene chain in the (self-assembled) A6/6 is not altered by adding A6/6 to the lipid. The isotropic dynamics of this chain still persist in the mixture. This observation again supports the conclusion that A6/6 is not inserted into the membrane (where the EO chains could potentially become immobilized by interaction with the headgroup region) but is rather located at the edges of the aggregates. This model is supported by solid-state NMR measurements, where we found that the A6/6 molecules do not modify the anisotropic motion of the lipid and therefore are not inserted into the membrane but are rather, possibly transiently, attached to the edges of the formed aggregates.

Our results, in particular the observation of identical lipid order parameters, demonstrate that the effects visible in the DSC curves (Figure 1) are only due to surface or edge effects. Thus, the NMR measurements confirm the model presented in Scheme 3, where A6/6 only stabilizes the edges of the formed bicelles when it is added to DPPC.

CONCLUSIONS

The aim of this work was to present the results of the investigation of the interactions of the facial amphiphile A6/6 with the lipid DPPC. A6/6 is surface active and can be easily suspended in water. The imaging techniques negative staining TEM and cryo-TEM gave information on the aggregation behavior of pure A6/6 and mixtures of A6/6 with the lipid DPPC in aqueous suspensions, respectively. For A6/6, we found by negative staining TEM lamellar folded sheets of very large dimensions and smooth edges indicating a well-ordered arrangement of the molecules within the sheets. At temperatures above the thermotropic transition observed by DSC, vesicles with diameters up to 500 nm and long stretched layered structures with a height of about 6 nm could be detected. The lamellae seemed to become more flexible at

dx.doi.org/10.1021/jp207996r | J. Phys. Chem. B 2012, 116, 4871–4878

higher temperature as the vesicular structures could be flattened and folded. Sonication reduced the size of the structures but had no major influence on the aggregation behavior except that in some cases fiber structures could also be observed.

For mixtures of DPPC with A6/6 at a ratio of 10:1, DSC indicated the formation of a stable complex of lipid with A6/6 as the transition temperature was increased. In the TEM images, we could observe flat hexagonal structures of constant thickness and diameters between 50 and 200 nm. The hexagonal appearance is probably induced by the regular packing of the alkyl chains of the lipids in the gel phase. Cryo-TEM images showed that the hexagonal structures are indeed flat objects. We concluded that these mixed aggregate structures are bicellar-like objects. We propose that the lipid bilayer patches are covered at the edges by the nearly T-shaped molecules leading to a microsegregation of lipid and A6/6. From DLS measurements, we could deduce that the particle size of the A6/6-DPPC aggregates changes only slightly with increasing A6/6 content. All the aggregates are surprisingly stable in their size over a wide temperature range and are also stable against aggregation after a long time storage at 4 °C for months. At present, we have not exploited the possibilities of these new bicellar-like systems for the incorporation of proteins and for investigations of membrane proteins by NMR with magnetically aligned samples and under static conditions. The advantages of this system could be lying in the low solubility of A6/6 in water, which prevents fast exchange of the molecule between the aggregate and water, and the therefore long-term stability of the bicellar aggregates. The disadvantages may lie in the more complicated preparation procedure of the samples including sonication. Further investigations in this direction are needed.

■ ASSOCIATED CONTENT

Supporting Information

Additional AFM data. This material is available free of charge via the Internet at http://pubs.acs.org.

■ AUTHOR INFORMATION

Corresponding Author

*Tel.: +49-345-5525850. Fax: +49-345-5527157. E-mail: alfred.blume@chemie.uni-halle.de.

Notes

The authors declare no competing financial interest.

■ ACKNOWLEDGMENTS

We thank the Deutsche Forschungsgesellschaft for financial support through the Forschergruppe FOR 1145 (TP 1, TP 4, and TP 5).

■ REFERENCES

(1) Chen, B.; Baumeister, U.; Pelzl, G.; Das, M. K.; Zeng, X.; Ungar, G.; Tschierske, C. *J. Am. Chem. Soc.* **2005**, *127*, 16578−16591.
(2) Stöckl, M. T.; Herrmann, A. *Biochim. Biophys. Acta* **2010**, *1798*, 1444−1456.
(3) Blume, A. *Thermochim. Acta* **1991**, *193*, 299−347.
(4) Bhattacharya, S.; Biswas, J. *Langmuir* **2010**, *26*, 4642−4654.
(5) Miyazaki, M.; Tajima, Y.; Handa, T.; Nakano, M. *J. Phys. Chem. B* **2010**, *114*, 12376−12382.
(6) Matsumori, N.; Murata, M. *Nat. Prod. Rep.* **2010**, *27*, 1480−1492.
(7) Sanders, C. R.; Prosser, R. S. *Structure* **1998**, *6*, 1227−1234.
(8) Shapiro, R. A.; Brindley, A. J.; Martin, R. W. *J. Am. Chem. Soc.* **2010**, *132*, 11406−11407.
(9) Cho, H. S.; Dominick, J. L.; Spence, M. M. *J. Phys. Chem. B* **2010**, *114*, 9238−9245.
(10) Beck, P.; Liebi, M.; Kohlbrecher, J.; Ishikawa, T.; Rüegger, H.; Fischer, P.; Walde, P.; Windhab, E. *Langmuir* **2010**, *26*, 5382−5387.
(11) Rodríguez, G; Rubio, L.; Cócera, M.; Estelrich, J.; Pons, R.; de la Maza, A.; López, O. *Langmuir* **2010**, *26*, 10578−10584.
(12) Dürr, U. H. N.; Waskell, L.; Ramamoorthy, A. *Biochim. Biophys. Acta* **2007**, *1768*, 3235−3259.
(13) Ramamoorthy, A. *Solid State Nucl. Magn. Reson.* **2009**, *35*, 201−207.
(14) Tschierske, C. *J. Mater. Chem.* **2001**, *11*, 2647−2671.
(15) Tschierske, C. *Chem. Soc. Rev.* **2007**, *36*, 1930−1970.
(16) Chen, B.; Zeng, X. B.; Baumeister, U.; Diele, S.; Ungar, G.; Tschierske, C. *Angew. Chem., Int. Ed.* **2004**, *43*, 4621−4625.
(17) Schröter, J. A.; Plehnert, R.; Tschierske, C.; Katholy, S.; Janietz, D.; Penacorada, F.; Brehmer, L. *Langmuir* **1997**, *13*, 796−800.
(18) Plehnert, R.; Schröter, J. A.; Tschierske, C. *Langmuir* **1998**, *14*, 5245−5249.
(19) Plehnert, R.; Schröter, J. A.; Tschierske, C. *Langmuir* **1999**, *15*, 3773−3781.
(20) Broniatowski, M.; Flasiński, M.; Dynarowicz-Łątka, P.; Majewski, J. *J. Phys. Chem. B* **2010**, *114*, 9474−9484.
(21) Kim, H. I.; Kim, H.; Shin, Y. S.; Beegle, L. W.; Goddard, W. A.; Heath, J. R.; Kanik, I.; Beauchamp, J. L. *J. Phys. Chem. B* **2010**, *114*, 9496−9503.
(22) Garidel, P.; Blume, A. *Chem. Phys. Lipids* **2005**, *138*, 50−59.
(23) Chimote, G.; Banerjee, R. J. *Biomed. Mater. Res., A* **2010**, *94 B*, 1−10.
(24) Cobo, M.; Achilles, A.; Reichert, D.; deAzevedo, E.; Saalwächter, K. *J. Magn. Res.* **2012**, submitted.
(25) Aussenac, F.; Laguerre, M.; Schmitter, J.; Dufourc, E. *Langmuir* **2003**, *19*, 10468−10479.
(26) Munowitz, M.; Griffin, R.; Bodenhausen, G.; Huang, T. *J. Am. Chem. Soc.* **1981**, *103*, 2529−2533.
(27) Gullion, T.; Schaefer, J. *J. Magn. Reson.* **1989**, *81*, 196−200.
(28) Hong, M.; Schmidt-Rohr, K.; Zimmermann, H. *Biochemistry* **1996**, *35*, 8335−8341.
(29) Bielecki, A.; Burum, D. *J. Magn. Reson. A* **1995**, *116*, 215−220.
(30) VanGeet, A. *Anal. Chem.* **1968**, *40*, 2227−2229.
(31) Dvinskikh, S. V.; Castro, V.; Sandstrom, D. *Magn. Reson. Chem.* **2004**, *42*, 875−881.
(32) Heerklotz, H. *J. Phys.: Condens. Matter* **2004**, *16*, R441−R467.
(33) Koynova, R.; Caffrey, M. *Biochim. Biophys. Acta* **1998**, *1376*, 91−145.
(34) Blume, A. *Biochim. Biophys. Acta* **1979**, *557*, 32−44.
(35) Prehm, M; Liu, F.; Zeng, X.-B.; Ungar, G.; Tschierske, C. *J. Am. Chem. Soc.* **2011**, *133*, 4906−4916.
(36) Optical investigation of the related T-shaped amphiphile A4/4 in a lyotropic system with formamide has indicated a transition from an optically uniaxial lamellar phase at higher temperature to a biaxial lamellar phase at lower temperature.[1] This is in line with the assumptions made for the temperature-dependent organization of A6/6 in the sheetlike aggregates.
(37) Garidel, P.; Fölting, B.; Schaller, I.; Kerth, A. *Biophys. Chem.* **2010**, *150*, 144−156.
(38) Pérez-Lara, A.; Ausili, A.; Aranda, F. J.; de Godos, A.; Torrecillas, A.; Corbalán-García, S.; Gómez-Fernández, J. C. *J. Phys. Chem. B* **2010**, *114*, 9778−9786.
(39) Dvinskikh, S. V.; Yamamoto, K.; Dürr, U. H. N.; Ramamoorthy, A. *J. Magn. Reson.* **2007**, *184*, 228−235.
(40) Yamamoto, K.; Soong, R.; Ramamoorthy, A. *Langmuir* **2009**, *25*, 7010−7018.
(41) Schmidt-Rohr, K.; Spiess, H. W. *Macromolecules* **1991**, *24*, 5288−5293.